



Contents lists available at ScienceDirect

Chemical Engineering Research and Design

journal homepage: www.elsevier.com/locate/cherdiChemE
ADVANCING
CHEMICAL
ENGINEERING
WORLDWIDE

Globally optimal distillation tray design using a mathematical programming approach

Aline R.C. Souza^a, Miguel J. Bagajewicz^{a,b,c}, André L.H. Costa^{a,*}

^a Rio de Janeiro State University (UERJ), Rua São Francisco Xavier, 524, Maracanã, CEP 20550-900, Rio de Janeiro, RJ, Brazil

^b School of Chemical, Biological and Materials Engineering, University of Oklahoma, Norman, Oklahoma, 73019, USA

^c Federal University of Rio de Janeiro (UFRJ), Escola de Química, CT, Bloco E, Ilha do Fundão, CEP 21949-900, Rio de Janeiro, RJ, Brazil

ARTICLE INFO

Article history:

Received 26 September 2021

Received in revised form 24 January 2022

Accepted 25 January 2022

Available online 29 January 2022

Keywords:

Distillation

Optimization

Design

ABSTRACT

This article presents the optimization of the design of distillation column trays. We develop a mixed-integer nonlinear optimization model, which we solve using mathematical programming. The objective of this formulation is to size all geometric variables of the tray. Two possible alternative objective functions are tested: column cost and column mass. The utilization of the proposed approach is illustrated through a design example from the literature. In this example, the optimal result obtained through the proposed approach is compared with the one obtained following the spirit of a traditional heuristic design procedure employed in process equipment design textbooks. The comparison indicates a reduction of both objective functions tested as compared to the result of the heuristic procedure.

© 2022 Institution of Chemical Engineers. Published by Elsevier Ltd. All rights reserved.

1. Introduction

In the United States, it is estimated that there are more than 40,000 distillation columns in operation, accounting for 90 % of the separation and purification processes. It is estimated that the capital invested in these systems is around US\$ 8 billion (Humphrey, 1995). Because the costs associated with this equipment are high, a considerable number of papers have addressed the optimal design of distillation columns. The main focus of these procedures is to optimize the column diameter, the number of trays, and the reflux ratio to minimize the total annualized cost.

Several different mathematical programming approaches were used to address this design problem: nonlinear programming (NLP) (Dowling and Biegler, 2015; Yeoh and Hui, 2021), mixed-integer nonlinear programming (MINLP) (Viswanathan and Grossmann, 1993; Kong and Maravelias, 2019), and generalized disjunctive programming (GDP) (Yeomans and Grossmann, 2000). Additionally, a combination of math-

ematical programming and commercial simulators was proposed by Caballero et al. (2005) and Caballero (2015).

Aiming at avoiding convergence drawbacks and local optimality problems associated with mathematical programming, some authors proposed the utilization of stochastic optimization methods for the solution of the aforementioned optimal design problem. Different techniques were tested, such as, particle swarm optimization (PSO) (Javaloyes-Antón et al., 2013), genetic algorithms (GA) (Ibrahim et al., 2017) and differential evolution (DE) associated with parallel computing (Lyu et al., 2021).

In all the aforementioned approaches, the dimensions of the column internals, namely, tray spacing, weir length, weir height, etc., have been not included. The traditional approach for the design of distillation column trays is based on trial and verification schemes, as depicted in several textbooks: Fair (1963), Wankat (1988), Kister (1992), Chuang and Nandakumar (2000), and Towler and Sinnott (2013). These schemes are considered reliable, but they depend on the designer's experience to attain a feasible choice of the tray geometric dimensions, with no guarantee that the solution found will feature the lowest cost. We know of only two works that employ optimization techniques for identifying the optimal set of tray dimensions: Ogboja and Kuye (1990) and Lahiri (2014, 2020). Ogboja and Kuye (1990) developed a sieve tray optimization

* Corresponding author.

E-mail address: andrehc@uerj.br (A.L.H. Costa).

<https://doi.org/10.1016/j.cherd.2022.01.036>

0263-8762/© 2022 Institution of Chemical Engineers. Published by Elsevier Ltd. All rights reserved.

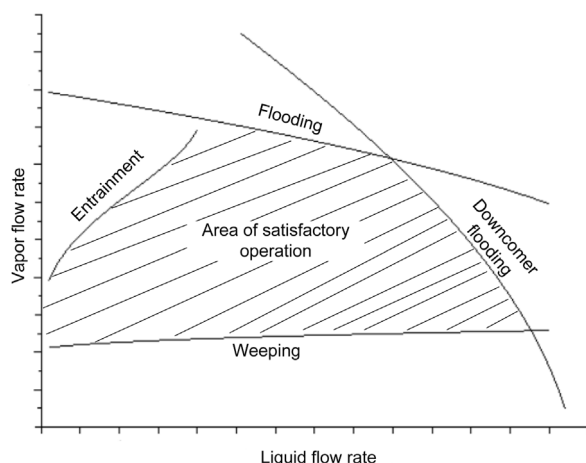


Fig. 1 – Tray performance diagram.

formulation, solved using the Complex method. The objective function is represented for the tray efficiency and the constraints are of geometrical and phenomenological origin. The decision variables are column diameter, spacing trays, tray thickness, weir length and height, hole diameter, and clearance height under the downcomer. As a way of validating the method, they used an exhaustive method that analyzes all sets of variables and determines their efficiency. Lahiri (2014, 2020) employed the PSO method together with the Aspen Plus simulator for the optimization of the distillation column including the specifications of the column tray. Lahiri (2014, 2020) considered complex tray configurations, such as multiple passes, sieve and valved trays, and segmental downcomer. The objective function to be minimized is the total annualized cost, considering the column capital costs and the costs associated with utility consumption.

In this article, we address the design of distillation column trays including the column diameter and all the geometric variables. We formulate the problem as a mixed-integer nonlinear model and we solve it using commercial global solvers (BARON and ANTIGONE). Previous approaches that addressed the tray design optimization employed local optimization methods (Ogboja and Kuye, 1990) or stochastic methods, which can escape local optima, but global optimality cannot be guaranteed (Lahiri, 2014, 2020). Additionally, the aforementioned works consider continuous variables, whereas the optimization method proposed in this work is based on discrete design variables. Indeed, the utilization of continuous variables to later use of commercial/standard geometric discrete values demands rounding procedures that can imply suboptimal or even infeasible solutions.

The article is organized as follows. Section 2 presents the tray operating limits that define the design constraints. Section 3 presents the dimensions of the sieve trays that are employed as optimization variables in the design problem. Sections 4 and 5 present the constraints and the objective functions of the Mixed Integer Nonlinear Model (MINLM), respectively. Section 6 presents the heuristic design procedure employed in the comparison of the results. Section 7 illustrates the performance of the proposed formulation and compares it with the heuristic procedure. The conclusions are finally presented in Section 8.

2. Tray operating range limits

In a given distillation column, the liquid and vapor flows must be contained within certain limits. Different authors characterize the phenomena associated with the operating limits of a tray differently, often using different nomenclatures. In this work, we will use the terminology adopted by Kister (1992). The operational limits that must be obeyed by the designer are flooding, entrainment, downcomer flooding, and weeping, as illustrated in Fig. 1. These operational limits origin the mathematical relations that compose the constraints of the optimization problem.

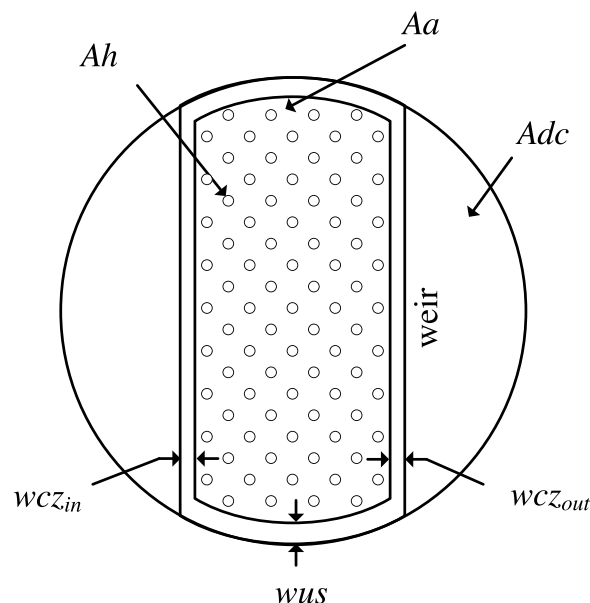


Fig. 2 – Sieve tray top view.

3. Sieve tray layout

Sieve trays feature different types of configurations for downcomer (segmental, circular, etc.), weir (straight, picket fence, etc.), and the number of passes (one or multiple passes, the latter option mostly employed for large diameters). Fig. 2 depicts the simplest configuration, which is the one we use in this work. The active area (A_a) is the tray area where liquid and vapor get in contact. The downcomer area (A_{dc}) is equivalent to the area of the inlet downcomer of the liquid flow from the tray above or the area of the outlet downcomer of the liquid flow to the tray below. The hole area (A_h) is the total area of the perforations on the tray.

Surrounding the active area, there are strips without holes. The almost rectangular strips, close to the downcomer slit and close to the weir, are referred to as “calming zones”. The calming zone region close to the downcomer, with width $w_{cz_{in}}$, aims to reduce the vorticity of the flow from the downcomer connected to the tray above. In turn, the calming zone region close to the weir, characterized by the width $w_{cz_{out}}$, aims to reduce instabilities of the flow close to the weir, thus reducing the turbulence associated to vapor bubbling through the liquid and allowing complete vapor-liquid separation so that bubbles are not carried towards the downcomer (Wankat, 1988). The circular gap with width w_{us} between the column shell and the active area is called “unperforated strip”. This gap is used for the support ring and does not have an explicitly hydraulic role (Towler and Sinnott, 2013).

Fig. 3 depicts a side view of the tray, showing the tray spacing (l_t), the weir height (h_w), the height of the liquid crest over the weir (h_{ow}), the clearance height under the downcomer (h_{ap}), the difference between weir and clearance height under the downcomer (h_{dwap}), and the downcomer backup height (h_b).

4. Tray design constraints

The optimization is focused on the design of the trays of a distillation column. It is assumed that the flow rates of the liquid and vapor and the corresponding physical properties were already previously calculated for each tray. These data

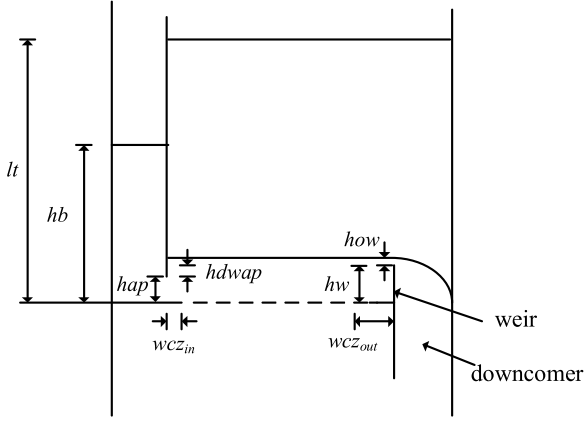


Fig. 3 – Tray side view.

are obtained from the distillation design, through a traditional approach based on heuristics or any of the optimization procedures available in the literature (see Section 1). Therefore, the model parameters associated with each tray sNt , represented here with a symbol $\hat{\cdot}$ on top, are: the liquid mass flow rate ($\hat{L}w_{sNt}$), the vapor mass flow rate ($\hat{V}w_{sNt}$), the density of the liquid ($\hat{\rho}^l_{sNt}$), the density of the vapor ($\hat{\rho}^v_{sNt}$), and the surface tension of the liquid ($\hat{\sigma}_{sNt}$).

Some additional parameters are calculated based on the values of the parameters listed above, as the liquid–vapor flow factor ($\hat{F}lv_{sNt}$) used in the Fair correlation (Fair, 1961):

$$\hat{F}lv_{sNt} = \frac{\hat{L}w_{sNt}}{\hat{V}w_{sNt}} \sqrt{\frac{\hat{\rho}^v_{sNt}}{\hat{\rho}^l_{sNt}}} \quad \forall sNt \quad (1)$$

and the residual pressure drop in the column tray ($\hat{h}r_{sNt}$), as proposed by Hunt et al. (1955):

$$\hat{h}r_{sNt} = \frac{12.5}{\hat{\rho}^l_{sNt}} \quad \forall sNt \quad (2)$$

Other specific parameters associated with the objective function are presented later.

4.1. Discrete representation of geometric variables

All the dimensions of the tray are represented by a set of discrete values. This representation is associated with the physical nature of some variables (e.g. hole layout: triangular or square); availability of commercial standards (e.g. tray thickness); or constructional patterns (e.g. manufacturing of mechanical pieces in inches or fractions of an inch).

The discrete representation of the design variables uses binary variables. Let x be a design variable that is associated with a set of possible values $\hat{p}x_i$. The selection of the discrete values $\hat{p}x_i$ is represented by the binary variables yx_i . Therefore, the variable x is related to the corresponding set of binary variables by:

$$x = \sum_i \hat{p}x_i yx_i \quad (3)$$

$$\sum_i yx_i = 1 \quad (4)$$

This representation is applied to the following set of variables associated with the tray design: column diameter (Dc),

hole diameter (dh), the difference between weir and clearance height under the downcomer ($hdwap$), weir height (hw), tray spacing (lt), weir length (lw), hole pitch (lp), tray thickness (tt), and hole layout (lay):

$$Dc = \sum_{sDc=1}^{sDcmax} p\hat{D}_{CsDc} yD_{CsDc} \quad (5)$$

$$dh = \sum_{sdh=1}^{sdhmax} p\hat{d}_{sdh} yd_{sdh} \quad (6)$$

$$hdwap = \sum_{shdwap=1}^{shdwapmax} p\hat{h}_{shdwap} yhd_{shdwap} \quad (7)$$

$$hw = \sum_{shw=1}^{shwmax} p\hat{h}_{shw} yhw_{shw} \quad (8)$$

$$lt = \sum_{slt=1}^{sltmax} p\hat{t}_{slt} ylt_{slt} \quad (9)$$

$$lw = \sum_{slw=1}^{slwmax} p\hat{l}_{slw} ylw_{slw} \quad (10)$$

$$lp = \sum_{slp=1}^{slpmax} p\hat{p}_{slp} ylp_{slp} \quad (11)$$

$$tt = \sum_{stt=1}^{sttmax} p\hat{t}_{stt} ytt_{stt} \quad (12)$$

$$lay = \sum_{slay=1}^{slaymax} p\hat{a}_{slay} ylay_{slay} \quad (13)$$

$$\sum_{sDc=1}^{sDcmax} yD_{CsDc} = 1 \quad (14)$$

$$\sum_{sdh=1}^{sdhmax} yd_{sdh} = 1 \quad (15)$$

$$\sum_{shdwap=1}^{shdwapmax} yhd_{shdwap} = 1 \quad (16)$$

$$\sum_{shw=1}^{shwmax} yhw_{shw} = 1 \quad (17)$$

$$\sum_{slt=1}^{sltmax} ylt_{slt} = 1 \quad (18)$$

$$\sum_{slw=1}^{slwmax} ylw_{slw} = 1 \quad (19)$$

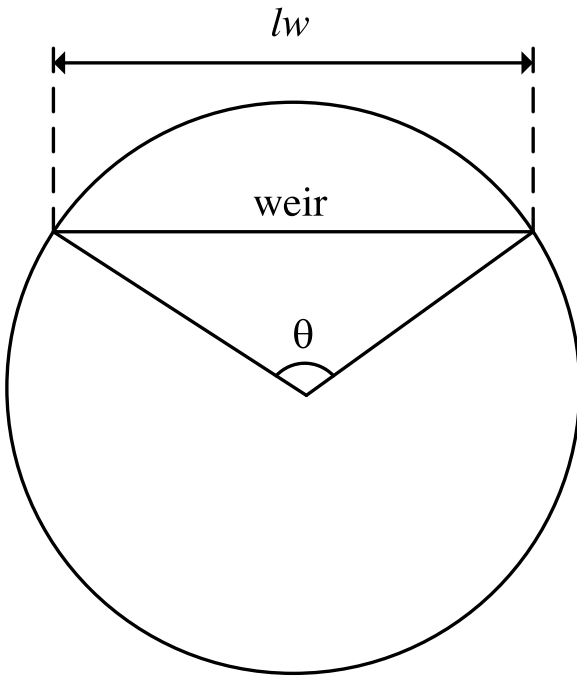


Fig. 4 – Graphical representation of the downcomer area evaluation.

$$\sum_{slp=1}^{slpmax} ylp_{slt} = 1 \quad (20)$$

$$\sum_{stt=1}^{sttmax} ytt_{stt} = 1 \quad (21)$$

$$\sum_{slay=1}^{slaymax} ylay_{slay} = 1 \quad (22)$$

4.2. Tray dimensions

The geometric equations are based on the sieve tray description presented in [Towler and Sinnott \(2013\)](#). The downcomer area is obtained by the difference between the circular sector area (A_{sector}) and the triangle area ($A_{triangle}$), as illustrated in [Fig. 4](#). Additionally, the vapor flow area (A_n) corresponds to the difference between the cross-sectional area of the column and the downcomer area.

Let θ be the weir angle, i.e. the central angle associated with the column circumference and the chord referring to weir length. Thus:

$$\theta - 2\arcsin(\delta) = 0 \quad (23)$$

where δ is the ratio between the weir length and the column diameter:

$$\delta D_c - lw = 0 \quad (24)$$

The area of the sector defined by the weir angle is:

$$A_{sector} - \frac{D_c^2 \theta}{8} = 0 \quad (25)$$

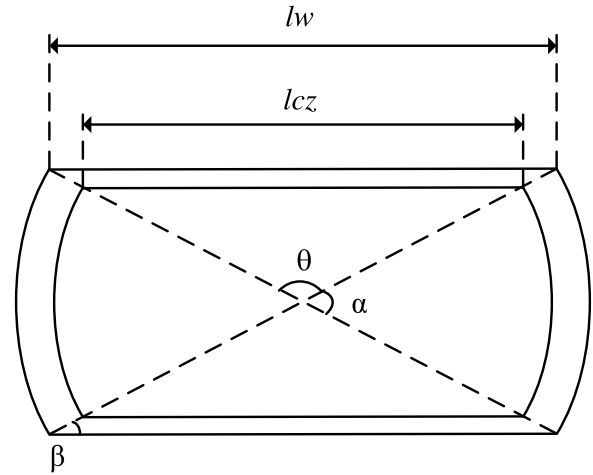


Fig. 5 – Calming zones and unperforated strip areas.

The area of the isosceles triangle is defined by the weir angle and the weir length as follows:

$$A_{triangle} - \frac{lw}{2} \sqrt{\left(\frac{D_c}{2}\right)^2 - \left(\frac{lw}{2}\right)^2} = 0 \quad (26)$$

Therefore, the total column area (A_c), the downcomer area (A_{dc}), and the vapor flow area (A_n) are given by:

$$A_c - \frac{\pi D_c^2}{4} = 0 \quad (27)$$

$$A_{dc} - A_{sector} + A_{triangle} = 0 \quad (28)$$

$$A_n - A_c + A_{dc} = 0 \quad (29)$$

The calming zone area (A_{cz}) is approximated by the area of two trapezoids, as illustrated in [Fig. 5](#), and is given by:

$$A_{cz} - \frac{(lcz_{in} + lw)}{2} \hat{w}cz_{in} - \frac{(lcz_{out} + lw)}{2} \hat{w}cz_{out} = 0 \quad (30)$$

where lcz_{in} and lcz_{out} are the lengths of the inlet and outlet calming zones. These lengths are related to other variables by:

$$lcz_{in} - lw + 2(wcz\beta_{in}) = 0 \quad (31)$$

$$lcz_{out} - lw + 2(wcz\beta_{out}) = 0 \quad (32)$$

where:

$$wc\beta_{in} \tan(\beta) - \hat{w}cz_{in} = 0 \quad (33)$$

$$wc\beta_{out} \tan(\beta) - \hat{w}cz_{out} = 0 \quad (34)$$

The angle β is the calming zone angle:

$$2\beta - \pi + \theta = 0 \quad (35)$$

Several references suggest a value for the width of the calming zone between 2 and 5 in, without differing inlet and outlet values ([Wankat, 1988](#); [Dutta, 2007](#); [Towler and Sinnott, 2013](#); [AMACS Process Tower Internals, 2020](#)). Then, we consider the width of the inlet and outlet calming zones ($\hat{w}cz_{in}$ and $\hat{w}cz_{out}$) equal to 0.050 m (2 in) in the proposed formulation.

The unperforated strip area (A_{us}) is determined using the angle of active area (α) and the width of the unperforated strip (w_{us}) (Towler and Sinnott, 2013):

$$A_{us} - w_{us} \alpha (D_c - w_{us}) = 0 \quad (36)$$

$$\alpha - \pi + \theta = 0 \quad (37)$$

The width of the unperforated strip varies according to the column diameter (AMACS Process Tower Internals, 2020), as follows:

$$w_{us} = \begin{cases} 0.0381, D_c \leq 0.7620 \\ 0.0508, 0.7620 < D_c \leq 1.6764 \\ 0.0635, 1.6764 < D_c \leq 3.8100 \\ 0.0762, 3.8100 < D_c \leq 5.9436 \\ 0.0889, 5.9436 < D_c \leq 7.4676 \\ 0.1143, D_c > 7.4676 \end{cases} \quad (38)$$

The reorganization of Eq. (38) into a set of inequalities using a set of auxiliary binary variables yields:

$$w_{us} - 0.0381 y_{wus_1} - 0.0508 y_{wus_2} - 0.0635 y_{wus_3} - 0.0762 y_{wus_4} - 0.0889 y_{wus_5} - 0.1143 y_{wus_6} = 0 \quad (39)$$

$$D_c - 0.7620 y_{wus_1} - 1.6764 y_{wus_2} - 3.8100 y_{wus_3} - 5.9436 y_{wus_4} - 7.4676 y_{wus_5} \leq 0 \quad (40)$$

$$D_c - 0.7620 y_{wus_2} - 1.6764 y_{wus_3} - 3.8100 y_{wus_4} - 5.9436 y_{wus_5} - 7.4676 y_{wus_6} - \hat{\varepsilon} \geq 0 \quad (41)$$

$$\sum_{s_{wus}=1}^6 y_{wus_{s_{wus}}} = 1 \quad (42)$$

where $\hat{\varepsilon} = 10^{-6}$.

The active area (A_a) corresponds to the cross-sectional area of the column minus the areas of the downcomers, unperforated strip, and calming zone.

$$A_a - A_c + 2 A_{dc} + A_{us} + A_{cz} = 0 \quad (43)$$

The total area of all the active holes (A_h) is a fraction of the active area, which depends on the hole layout:

$$A_h - k \varphi^2 A_a = 0 \quad (44)$$

where:

$$\varphi l_p - dh = 0 \quad (45)$$

$$k - 0.785 y_{lay_1} - 0.905 y_{lay_2} = 0 \quad (46)$$

where y_{lay_1} and y_{lay_2} are associated with the square and triangular layouts, respectively.

4.3. Geometric constraints

The weir length must be smaller than the column diameter:

$$l_w \leq D_c \quad (47)$$

The hole pitch must be higher than twice the hole diameter (Towler and Sinnott, 2013):

$$l_p \geq 2dh \quad (48)$$

Assuming that the tray holes are punched, the tray thickness cannot be higher than the hole diameter (Chuang and Nandakumar, 2000):

$$dh \geq tt \quad (49)$$

The range of the ratio between the hole area and the active area must be:

$$0.06 A_a \leq A_h \leq 0.16 A_a \quad (50)$$

The lower bound on Eq. (50) is necessary to use the Fair flooding correlation (Fair, 1961) and the upper bound avoids conditions where significant weeping and entrainment may coexist and the design equations may not apply (Chuang and Nandakumar, 2000).

Finally, to use the Fair flooding correlation, the following bound must be applied (Fair, 1961):

$$hw \leq 0.15 lt \quad (51)$$

4.4. Operational constraints

These constraints consist of equations representing the limits of flooding, entrainment, weeping, downcomer backup, and residence time in the downcomer.

4.4.1. Flooding

To avoid flooding, an upper bound on the vapor flow velocity is used:

$$u_{sNt} - 0.85 u_{flood_{sNt}} \leq 0 \quad \forall sNt \quad (52)$$

where u_n is the vapor flow velocity and u_{flood} is the flooding velocity, both based on the vapor flow area.

The vapor flow velocity can be evaluated as follows:

$$u_{sNt} A_n - \frac{V \dot{w}_{sNt}}{\rho \dot{v}_{sNt}} = 0 \quad \forall sNt \quad (53)$$

The determination of the flooding condition is given by Fair (1961):

$$u_{flood_{sNt}} - K1 Csb_{sNt} \sqrt{\frac{\hat{\rho} l_{sNt} - \hat{\rho} \dot{v}_{sNt}}{\hat{\rho} \dot{v}_{sNt}}} \left(\frac{\hat{\sigma}_{sNt}}{0.02} \right)^{0.2} = 0 \quad \forall sNt \quad (54)$$

where Csb is the Sounders-Brown coefficient.

In turn, the parameter $K1$ varies with the fraction of the hole area:

$$K1 = \begin{cases} 0.8, & 0.06 \leq k\varphi^2 \leq 0.08 \\ 0.9, & 0.08 \leq k\varphi^2 \leq 0.10 \\ 1.0, & 0.10 \leq k\varphi^2 \leq 0.16 \end{cases} \quad (55)$$

The parameter $K1$ had to be rearranged into inequalities using binary variables to represent the different options in purely algebraic form:

$$K1 - 0.8yK1_1 - 0.9yK1_2 - 1.0yK1_3 = 0 \quad (56)$$

$$k\varphi^2 - 0.08yK1_1 - 0.10yK1_2 - 0.16yK1_3 \leq 0 \quad (57)$$

$$k\varphi^2 - 0.06yK1_1 - 0.08yK1_2 - 0.10yK1_3 \geq 0 \quad (58)$$

$$\sum_{sK1=1}^3 yK1_{sK1} = 1 \quad (59)$$

Several authors have presented curve fitting of the Fair's correlation (Economopoulos, 1978; Lygeros and Magoulas, 1986; Ogboja and Kuye, 1990). The expression we use is the proposed by Ogboja and Kuye (1990):

$$Csb_{sNt} - 0.0129 - 0.1674lt - 0.0063Flv_{sNt} + 0.2686lt Flv_{sNt} + 0.008Flv_{sNt}^2 - 0.01448lt Flv_{sNt}^2 = 0 \quad \forall sNt \quad (60)$$

4.4.2. Entrainment

The constraint to avoid entrainment is represented by an upper bound on the fractional entrainment variable (ψ_{sNt}):

$$\psi_{sNt} - 0.1 \leq 0 \quad \forall sNt \quad (61)$$

The fractional entrainment can be estimated by the correlations proposed by Economopoulos (1978) or Ogboja and Kuye (1990). We choose to use the correlation of Ogboja and Kuye (1990):

$$\psi_{sNt} - \left\{ \exp \left[\begin{aligned} & -7.9196 + 1.0891Fflood_{sNt} \\ & - (0.0705 + 2.1916Fflood_{sNt}) \ln Flv_{sNt} \\ & + (0.046 - 0.605Fflood_{sNt} + 1.2669Fflood_{sNt}^2) \\ & - 0.9563Fflood_{sNt}^3 \end{aligned} \right] (\ln Flv_{sNt})^2 \right\} = 0 \quad \forall sNt \quad (62)$$

where $Fflood$ is the factor of flooding:

$$Fflood_{sNt} u_{flood_{sNt}} - u_{sNt} = 0 \quad \forall sNt \quad (63)$$

4.4.3. Weeping

The constraint to assure that the tray design will not be subjected to weeping is represented by a lower bound on the flow velocity throughout the tray holes:

$$u_{hsNt} - u_{hmin_{sNt}} \geq 0 \quad \forall sNt \quad (64)$$

where u_h is the vapor flow velocity throughout the tray holes and it can be calculated by:

$$u_{hsNt} Ah - \frac{\hat{V}w_{sNt}}{\hat{\rho}v_{sNt}} = 0 \quad \forall sNt \quad (65)$$

and the weeping point associated with the minimum vapor flow velocity (u_{hmin}) can be determined by the following correlation (Edulee, 1959):

$$u_{hmin_{sNt}} - \frac{K2_{sNt} - 0.9(25.4 - 10^3 dh)}{(\hat{\rho}v_{sNt})^2} = 0 \quad \forall sNt \quad (66)$$

where $K2$ is evaluated by the correlation proposed by Ogboja and Kuye (1990):

$$K2_{sNt} - 23.48 - 1.66 \ln [10^3 (hw + how_{sNt})] = 0 \quad \forall sNt \quad (67)$$

The height of the liquid crest over the weir (how) can be estimated using the Francis weir formula:

$$how_{sNt} - 750 \cdot 10^{-3} \left(\frac{\hat{L}w_{sNt}}{\hat{\rho}l_{sNt} lw} \right)^{\frac{2}{3}} = 0 \quad \forall sNt \quad (68)$$

4.4.4. Downcomer backup

The constraint to avoid flooding in the downcomer must impose an upper bound on the downcomer backup height:

$$hb_{sNt} - \frac{1}{2} (lt + hw) \leq 0 \quad \forall sNt \quad (69)$$

$$hb_{sNt} - hw - how_{sNt} - ht_{sNt} - hdc_{sNt} = 0 \quad \forall sNt \quad (70)$$

where ht is total tray head loss and hdc is head loss in the downcomer.

The total tray head loss is the sum of the head of clear liquid on the tray ($hw + how$) and the dry tray drop (hd):

$$ht_{sNt} - hw - how_{sNt} - hd_{sNt} - \hat{h}r_{sNt} = 0 \quad \forall sNt \quad (71)$$

The dry tray head loss is given by:

$$hd_{sNt} Co^2 - 51 \cdot 10^{-3} u_{hsNt}^2 \frac{\hat{\rho}v_{sNt}}{\hat{\rho}l_{sNt}} = 0 \quad \forall sNt \quad (72)$$

where Co is the orifice coefficient that can be estimated by the correlations proposed by Economopoulos (1978) or Ogboja and Kuye (1990). We choose to use the correlation of Ogboja and Kuye (1990):

$$Co - 0.6323 + 0.0255\omega - 0.1495\omega^2 - 0.777k\varphi^2 = 0 \quad (73)$$

where:

$$\omega dh = tt \quad (74)$$

Cicalese et al. (1947) estimated the head loss in the downcomer by:

$$hdc_{sNt} Aap - 166 \cdot 10^{-3} \left(\frac{\hat{L}w_{sNt}}{\hat{\rho}l_{sNt}} \right) = 0 \quad \forall sNt \quad (75)$$

where A_{ap} is the clearance area under the downcomer that can be determined by:

$$A_{ap} - h_{ap} l_w = 0 \quad (76)$$

The height of the clearance under the downcomer (h_{ap}) is given by:

$$h_{ap} - h_w + h_{dwap} = 0 \quad (77)$$

4.4.5. Residence time

The downcomer residence time must be enough for promoting vapor and liquid separation and preventing that the heavily aerated liquid be transported under the downcomer (Towler and Sinnott, 2013):

$$time_{sNt} - 3 \geq 0 \quad \forall sNt \quad (78)$$

where:

$$time_{sNt} - A_{dc} h_{b_{sNt}} \frac{\hat{\rho}_{l_{sNt}}}{\hat{L} \hat{w}_{sNt}} = 0 \quad \forall sNt \quad (79)$$

4.5. Variable bounds

Bounds on the design variables (D_c , dh , h_{dwap} , h_w , l_t , l_w , l_p , tt , and lay) are aggregated considering the available options associated with the tray manufacturing process, usual alternatives employed in practice and literature recommendations:

$$\hat{D}_{c_{min}} \leq D_c \leq \hat{D}_{c_{max}} \quad (80)$$

$$\hat{dh}_{min} \leq dh \leq \hat{dh}_{max} \quad (81)$$

$$h_{dwap_{min}} \leq h_{dwap} \leq h_{dwap_{max}} \quad (82)$$

$$\hat{h}_{w_{min}} \leq h_w \leq \hat{h}_{w_{max}} \quad (83)$$

$$\hat{l}_{t_{min}} \leq l_t \leq \hat{l}_{t_{max}} \quad (84)$$

$$\hat{l}_{w_{min}} \leq l_w \leq \hat{l}_{w_{max}} \quad (85)$$

$$\hat{l}_{p_{min}} \leq l_p \leq \hat{l}_{p_{max}} \quad (86)$$

$$\hat{tt}_{min} \leq tt \leq \hat{tt}_{max} \quad (87)$$

$$\hat{lay}_{min} \leq lay \leq \hat{lay}_{max} \quad (88)$$

Bounds are also imposed to the variables W_{shell} and t_{wall} that appears in the objective function to represent the mass of the column shell and the column thickness (Towler and Sinnott, 2013):

$$W_{shell_{min}} \leq W_{shell} \leq W_{shell_{max}} \quad (89)$$

$$t_{wall_{min}} \leq t_{wall} \leq t_{wall_{max}} \quad (90)$$

Finally, bounds on the following variables are related to their physical nature:

$$0.0381 \text{ m} \leq w_{us} \leq 0.143 \text{ m} \quad (91)$$

$$0.8 \leq K_1 \leq 1.0 \quad (92)$$

$$0 \leq \beta \leq \frac{\pi}{2} \quad (93)$$

5. Objective function

The optimization seeks to minimize the capital cost associated with the distillation column. An equation for evaluation of the capital cost of a distillation column, provided by Towler and Sinnott (2013), is employed as the objective function:

$$\text{Min } C_{total} = (130 + 440 D_c^{1.8}) \hat{N}_t + 11600 + 34 W_{shell}^{0.85} \quad (94)$$

where \hat{N}_t is the number of trays and W_{shell} is the mass of the column shell. This equation is valid for carbon steel columns with $0.5 \text{ m} \leq D_c \leq 5.0 \text{ m}$ and $160 \text{ kg} \leq W_{shell} \leq 250,000 \text{ kg}$.

The mass of the column shell is given by:

$$W_{shell} - \pi \rho_{shell} D_c H_c t_{wall} = 0 \quad (95)$$

where ρ_{shell} is the density of the shell material and H_c is the height of the column between tangent lines, given by:

$$H_c - \hat{N}_t l_t = 0 \quad (96)$$

The column wall thickness depends on the column diameter:

$$t_{wall} - \sum_{sD_c=1}^{sD_{c_{max}}} P t_{wall_{sD_c}} y_{D_{c_{sD_c}}} = 1 \quad (97)$$

where $P t_{wall_{sD_c}}$ is the thickness value corresponding to the mechanical design associated with the column diameter related to the binary variable $y_{D_{c_{sD_c}}}$.

Another alternative of the objective function consists in minimizing the mass of the distillation column (W_{total}), considering the mass of the column (W_{column}) and trays (W_t).

$$\text{Min } W_{total} = W_{column} + W_t \hat{N}_t \quad (98)$$

The mass of the column is given by (Towler and Sinnott, 2013):

$$W_{column} - \hat{C}_w \pi \rho_{shell} D_m (H_c + 0.8 D_m) t_{wall} = 0 \quad (99)$$

where \hat{C}_w is a factor responsible for the mass of nozzles, manways, internal supports, etc, (assumed equal to 1.15), and D_m is the mean diameter of the column. The mean diameter is given by:

$$D_m - D_c - t_{wall} = 0 \quad (100)$$

The mass of the tray is determined by the volume of the tray deck (V_t) and the volume of the weir together with the downcomer (V_{wdc}).

$$W_t - (V_t + V_{wdc}) \hat{\rho}_t = 0 \quad (101)$$

where $\hat{\rho}_t$ is the specific mass of tray material.

The V_{wdc} is given by a rectangular plate:

$$V_{wdc} - (h_w + tt + H_{dc}) tt l_w = 0 \quad (102)$$

where H_{dc} is the height of the downcomer:

$$H_{dc} - l_t + h_{ap} = 0 \quad (103)$$

The volume for each tray is given by the area of the column minus the areas of the downcomer and holes.

$$V_t - (A_c - A_{dc} - A_h) t_t = 0 \quad (104)$$

6. Heuristic design procedure

Aiming at comparing the performance of the proposed approach for the sizing of distillation columns with traditional schemes, a heuristic procedure based on Towler and Sinnott (2013) is presented in this section.

The original design discussion in Towler and Sinnott (2013) does not describe in detail all the steps of the procedure, deferring implicitly to the designer certain decisions. We seek to provide a design scheme that could be as systematic as possible, devoid as much as possible from calls to vague changes. However, some decisions from a practitioner are still needed.

In the next paragraphs, we present an analysis based on the literature about the selection of certain dimensions of the sieve tray. The values presented here serve as initial guesses in the design procedure.

- Tray spacing: Towler and Sinnott (2013) do not provide guidelines. Kister (1992) shows a range for tray spacing from 8 in until 36 in, but adopting 24 in, other authors (Fair, 1963; Wankat, 1988) agree with him. Therefore, we settle in adopting 24 in as a first choice.
- Downcomer area: we use the direct recommendation given by Towler and Sinnott (2013), that is, 12% of the total column area as the starting point.
- Vapor velocity: The recommendation provided by Towler and Sinnott (2013) and Fair (1963) is to pick a vapor velocity equal to 85% of the flooding velocity. Other values used are 80 % by Kister (1992) and Couper et al. (2012) and 75 % by Wankat (1988). We adopt the largest value of the literature.
- Hole area: The hole area is initially estimated at 10 % of the active area by different authors (Wankat, 1988; Kister, 1992; Towler and Sinnott, 2013; Couper et al., 2012). We use this choice as the initial guess.
- Tray thickness: Towler and Sinnott (2013) do not recommend the use of any specific value, but they use 5 mm in their example. We choose 3.4 mm, which is the smallest thickness used in the literature (Kister, 1992; Chuang and Nandakumar, 2000).
- Hole diameter: Towler and Sinnott (2013) offer the following limits: $0.0025 \text{ m} \leq d_h \leq 0.012 \text{ m}$. They also state that the diameter is subject to a limit related to the tray thickness ($d_h/t_t \geq 1$). Towler and Sinnott (2013) do not offer a criterion and in their example, they use 5 mm, pretty much in the middle of the range. For Kister (1992) the choice depends on the service, for clean services is 3/16 in, for fouling services is 1/2 in. Other authors also choose 3/16 in (Fair, 1963; Wankat, 1988; Kooijman and Taylor, 2006). Engel (2020) indicates that small holes are preferable due to hydraulic reasons, but penalize the fabrication costs. We adopt the valor shared by most of the literature 3/16 in (4.8 mm) and later change it if there is a need to do it.
- Weir height: For Towler and Sinnott (2013) the choice depends on the operation, for columns operating above

atmospheric pressure is $0.040 \text{ m} \leq h_w \leq 0.090 \text{ m}$, for vacuum operation is $0.006 \text{ m} \leq h_w \leq 0.012 \text{ m}$. It must be $h_w < 0.15 l_t$. Other authors also choose 2 in (0.051 m) (Fair, 1963; Wankat, 1988; Kister, 1992; Kooijman and Taylor, 2006; Couper et al., 2012; Towler and Sinnott, 2013). Larger heights have a significant effect on pressure drop, so from this point of view, smaller values should be preferred. We adopt the valor shared by most of the literature.

- Difference between weir and clearance height under the downcomer: Towler and Sinnott (2013) consider the following values $0.005 \text{ m} \leq h_{dwap} \leq 0.010 \text{ m}$. Kister (1990) explains that the largest value is to avoid an excessive increase in the pressure drop, which would cause a downcomer backup flooding. The smallest value is adopted to avoid that the vapor flows up the downcomer. Other authors specify certain valor (Fair, 1963; Kister, 1990; Kooijman and Taylor, 2006) for this variable as 10 mm. We decided to adopt this value.

Our procedure mimics the one suggested by Towler and Sinnott (2013) and complemented with our considerations and is the following:

Step 1: Data collection: Obtain flow rates and physical properties of the vapor and liquid streams of two representative trays, one from the rectifying section and another from the stripping section (one can extend this exercise to all trays in each section and then somehow find compromise solutions for each section, but we do not pursue this here, thus sticking to the classical recommendation).

Step 2: Perform preliminary specifications: Select values of tray spacing, downcomer area fraction of total area (FA_{dc}), and flooding fraction to determine the column diameter (0.85).

Step 3: Determine the column diameter corresponding to both trays (rectifying and stripping section representatives) based on flooding considerations:

$$D_c = \left[\frac{4\hat{V}_w}{\pi \cdot 0.85 u_{flood} \hat{\rho}_v (1 - FA_{dc})} \right]^{0.5} \quad (105)$$

Because only one diameter is sought after (unless there are serious mismatches and the column needs more than one diameter), the largest of both diameters is picked.

The column diameter must be higher than 0.60 m to avoid difficulties of installation (Towler and Sinnott, 2013). If the value obtained is smaller than 0.60 m, then return to Step 2 and reduce the tray spacing or increase the downcomer area fraction. We offer the following rationale. If the diameter obtained violates the above inequality by a small amount, it is advisable to change the downcomer area criteria (increase 12 % by a small amount), to make the calculated diameter fit the inequality. If the diameter obtained is far away from the limit established by the inequality, that is, it is very small in comparison, then it is advisable to reduce the tray spacing.

Step 4: Finalize tray geometry specifications

- Evaluate an initial estimative of the active area:

$$A_a = A_c - 2A_{dc} \quad (106)$$

- Hole area: use 10 % of the active area or other value if needed for respecting the constraint for the use of the Fair correlation $0.06 < A_h/A_a < 0.16$ (Fair, 1963).

Table 1 – Operational parameters of the example.

Parameters/Tray	1	2	3	4	5	6	7	8	9
$\dot{L}w$ (kg/s)	0.82	0.80	0.78	0.76	0.72	0.66	0.51	3.12	2.78
$\dot{V}w$ (kg/s)	1.50	1.48	1.46	1.43	1.40	1.34	1.18	1.02	0.68
$\hat{\rho}l$ (kg/m ³)	753.76	754.64	755.64	756.92	758.84	762.57	776.27	873.01	900.73
$\hat{\rho}v$ (kg/m ³)	2.10	2.09	2.07	2.04	2.01	1.95	1.78	1.61	1.02
$\hat{\sigma}$ (N/m) $\times 10^3$	22.28	23.20	24.21	25.45	27.21	30.28	38.60	59.14	60.79

- c) Tray thickness: We use the smallest value (3.4 mm) as discussed above.
- d) Hole diameter: We use the recommendations discussed above (4.8 mm). Because the thickness has already been set in the previous step, we choose a hole diameter that respects the limit established by the thickness ($dh/tt \geq 1$).
- e) Weir height: We use 51 mm (2 in) as discussed above.
- f) Difference between weir and clearance height under the downcomer: We use the largest value (10 mm) as discussed above.
- g) Weir length: It is determined based on a graphical relation present in [Towler and Sinnott \(2013\)](#) ($lw < Dc$).

Step 5: Check the weeping safety factor (Eq. (64)); if unsatisfactory, return to Step 4, reducing the hole area.

Step 6: Check the downcomer backup safety factor (Eq. (69)). If unsatisfactory return to Step 4, increasing the hole area, reducing the downcomer area, and/or increasing the tray spacing.

Step 7: Check the downcomer residence time safety factor (Eq. (78)); if unsatisfactory, return to Step 4, reducing the hole area or increasing the downcomer area.

Step 8: Specify tray layout details:

- a) Width of the calming zone: We choose 0.050 m for the input and output calming zones (the same values adopted in our optimization model).
- b) Width of unperforated areas: We choose what we use in our model (Eq. (38)).
- c) Hole layout: We adopt the option shared by most of the literature as triangular layout ([Fair, 1963](#); [Wankat, 1988](#); [Kister, 1992](#); [Kooijman and Taylor, 2006](#); [Towler and Sinnott, 2013](#)).
- d) Recalculate the active area considering calming zone area and unperforated strip area:

$$Aa = Ac - 2Adc - Acz - Aus \quad (107)$$

Step 9: Determine the hole pitch by Eq. (108) and check the safety factor ($lp \geq 2dh$), if unsatisfactory, then return to Step 4, increasing the hole diameter.

$$lp = dh \left(\frac{0.905Aa}{Ah} \right)^{0.5} \quad (108)$$

Step 10: Check the flooding safety factor (Eq. (52)), if unsatisfactory, then return to Step 4, increasing the tray spacing.

Step 11: Check the entrainment safety factor (Eq. (61)), if unsatisfactory then return to Step 4, increasing the tray spacing. Otherwise, stop.

Other procedures and equations used in the literature exist and they are all based on trial and verification steps. The intervention of an experienced designer becomes important in Steps 2, 4, and 8 to adequately select the values of the design variables to be verified. In the verification steps, a check is

made to see if the design is feasible or not (Steps 5, 6, 7, 9, 10, and 11).

7. Results

The performance of the proposed MINLP procedure for the optimal design of distillation columns trays is illustrated by the solution of an example from the literature ([Towler and Sinnott, 2013](#)) together with a comparison with the corresponding results of the heuristic procedure.

The example considers a distillation column with an aqueous waste stream as feed, where it is desired to recover acetone. The feed is a stream with 454.5 kmol/h of a mixture containing 10 % of acetone (all compositions are expressed here using a molar basis). The top stream must contain 95 % of acetone and the bottom stream must not contain more than 1 % of acetone. The example considers ten equilibrium stages with a total condenser. The operation pressure is 1 atm.

The column was simulated in the Aspen Plus software using the property method UNIQUAC, which employs the Redlich-Kwong equation of state ([Redlich and Kwong, 1979](#)) and the UNIQUAC activity coefficient model ([Abrams and Prausnitz, 1975](#)). The reflux ratio is 1.24 and the feed tray corresponds to stage 8. The results of the simulation for the nine ideal stages are presented in [Table 1](#) (the equilibrium stage 10 corresponds to the kettle reboiler).

The overall efficiency was assumed to be equal to 60 %. Excluding the reboiler, the nine ideal stages correspond to 15 real stages. This value was employed for the evaluation of the column height in the objective function. The column material was carbon steel ($\rho_w = 7900$ kg/m³).

[Table 2](#) displays the standard alternatives of the discrete geometric variables employed in the design problem. This set of options corresponds to a search space composed of 7,931,520 candidates (total number of possible combinations of the values of the design variables). The lower and upper bounds are outlined by Eqs. (80–88) correspond to the minimum and maximum values displayed in [Table 2](#). The lower and upper bounds on the variable W_{shell} are $W_{shell_{min}} = 160$ and $W_{shell_{max}} = 250000$, according to the validity range of the correlation in Eq. (94).

The column diameters vary between 0.6096 m (24 in) and 4.826 m (190 in), the diameter lower bound being necessary to avoid difficulties of installation ([Towler and Sinnott, 2013](#)), and the upper bound is related to the maximum that the column cost equation allows (Eq. (94)) ([Towler and Sinnott, 2013](#)). The discrete values of the diameters employed in the optimization were selected in such a way that the differences between them increase as the diameter increases.

The diameters of the holes correspond to the commercial standardization of drills ([Oberg et al., 2004](#)). Their limits are chosen to respect the Fair entrainment correlation limits ([Fair, 1961](#)), that is, between 1.6 mm (1/16 in) and 6.4 mm (1/4 in). Moreover, hole diameters must respect the geometric constraints (Eqs. (48–49)). The limits of the variables hd_{wap} , hw

Table 2 – Discrete values of the design variables.

Variables	Discrete values																
Dc (m)	0.61	0.76	0.91	1.07	1.27	1.47	1.68	1.93	2.18	2.44	2.74	3.05	3.35	3.71	4.06	4.42	4.83
dh (mm)	3.60	4.00	4.40	4.80	5.20	5.60	6.00	6.40									
hdwap (mm)	5.00	6.00	7.00	8.00	9.00	10.0											
hw (cm)	3.81	4.44	5.08	5.71	6.35	6.98	7.62	8.25	8.89								
lt (m)	0.15	0.23	0.31	0.47	0.62	0.91											
lw (m)	0.41	0.66	0.91	1.17	1.42	1.68	1.93	2.18	2.44	2.69	2.95	3.20	3.45	3.71	3.96		
lp (mm)	9.00	12.0	15.0	18.0	21.0	24.0											
tt (mm)	3.40																
lay	Square		Triangular														

Table 3 – Shell thickness for each column diameter.

Dc (m)	0.61	0.76	0.91	1.07	1.27	1.47	1.68	1.93	2.18	2.44	2.74	3.05	3.35	3.71	4.06	4.42	4.83
twall (mm)	5	5	5	7	7	7	7	7	9	9	10	12	12	12	12	12	12

Table 4 – Results.

	MINLP – Minimization of the column cost	MINLP – Minimization of the column mass	Heuristics
Ctotal (\$)	28,915.69	28,915.69	31,822.12
Wtotal (kg)	1,339.42	1,335.52	1,831.70
Dc (m)	0.9144	0.9144	0.7307
dh (m)	0.0036	0.0036	0.0048
hdwap (m)	0.008	0.005	0.010
hw (m)	0.0381	0.0381	0.0508
lt (m)	0.4572	0.4572	0.9144
lw (m)	0.6604	0.6604	0.5550
lp (m)	0.009	0.009	0.011
lay	Square	Triangular	Triangular

and lt were established based on their corresponding typical values (Towler and Sinnott, 2013). Finally, the limits of the variables lw and lp were generated from the limits of the variables Dc and dh according to the relations suggested by Towler and Sinnott (2013):

$$0.6 \leq \frac{lw}{Dc} \leq 0.85 \quad (109)$$

$$2.5 \leq \frac{lp}{dh} \leq 4.0 \quad (110)$$

The values of the column shell thickness related to each column diameter alternative are shown in Table 3, according to Towler and Sinnott (2013). The lowest and highest values of thicknesses are employed as lower and upper bounds on the variable t_{wall} .

The MINLM formulation of the design optimization problem was solved by MINLP procedures using the GAMS software interface (version 24.7.1) and the global optimization solvers ANTIGONE (version 1.1) and BARON (version 16.3.4).

Because ANTIGONE and BARON do not accept trigonometric functions, Taylor series expansions to represent those functions were used (Gradshteyn and Ryzhik, 2015):

$$\tan x = \sum_{k=1}^{\infty} \frac{2^{2k} (2^{2k} - 1)}{(2k)!} |B_{2k}| x^{2k-1}, \quad |x| < \frac{\pi}{2} \quad (111)$$

$$\arcsin x = \sum_{k=0}^{\infty} \frac{(2k)!}{2^{2k} (k!)^2 (2k+1)} x^{2k+1} \quad (112)$$

where Be is the Bernoulli number obtained from Plouffe (2001). The series representing the tangent function was evaluated using 81 terms and the series of the arcsine function involved 14 terms, which have an error below 0.001.

The computational times associated with the optimization using the solver ANTIGONE were 73 s and 20 s for cost and mass as objective functions, respectively. The corresponding computational times using the solver BARON were 136 s and 36 s. These times were collected in a computer with an Intel Core i7 processor with 8 Gb of RAM.

The comparison of the solutions obtained using ANTIGONE and BARON indicates that BARON did not attain the global optimum in the minimization of the cost (the value of the objective function obtained using BARON was 13 % higher than the solution using ANTIGONE). The results obtained using ANTIGONE are displayed in Table 4, for different objective functions. These solutions are similar, exhibiting different masses: 1,339.42 kg for the cost objective function and 1,335.52 kg for the mass objective function. The total cost is the same (\$ 28,915.69) because the cost function is not detailed enough to be sensitive to the minor differences between these similar solutions.

The heuristic design procedure was also applied to the solution of the same design example. The details of the application of the heuristic procedure are present in the Supplementary Material, including all the candidates tested during the search. The final feasible solution found is also presented in Table 4. This solution is associated with a cost and a mass equal to \$ 31,822.12 and 1,831.70 kg, respectively.

The comparison of the optimal values of the objective function with the results obtained using the heuristic procedure indicates that the optimization attained a reduction of 9 % of the cost and 27 % of the mass of steel.

8. Conclusions

This paper presented a Mixed Integer Nonlinear Model solved using a MINLP procedure for the tray design of distillation columns. For a given set of flow rates and physical properties, the optimization determines the optimal value of the column diameter and all the dimensions of the trays. Two alternative objective functions were used: cost and mass. The method can be also extended for other internals (e.g. valve trays, bubble cap trays, etc.) or objective functions (e.g. more detailed cost functions based on mechanical design). Additionally, a step-by-step heuristic procedure, based on the literature, was

presented and used for comparison. Significant reductions were obtained in both objective functions.

Besides the advantages of the mathematical programming approach, the heuristic procedures have another disadvantage: they rely on experienced practitioners. Therefore, a novice engineer may obtain a more expensive solution than an experienced one. Comparatively, the application of the optimization approach is automatic and the least cost design is attained, no matter the experience of the user.

Conflict of interest

The authors declare that they have no known competing financial interests or personal relationships that could have appeared to influence the work reported in this paper.

Acknowledgments

Aline R. C. Souza thanks the Coordination for the Improvement of Higher Education Personnel (CAPES) for the scholarship. André L. H. Costa would like to thank the National Council for Scientific and Technological Development (CNPq) for the research productivity fellowship (Process 310390/2019-2) and the Rio de Janeiro State University through the Prociência Program. Miguel J. Bagajewicz would like to thank the Rio de Janeiro State University (Brazil) for its scholarship of Visiting Researcher - PAPD Program as well as the Federal University of Rio de Janeiro (Brazil) for its support.

Appendix A. Supplementary data

Supplementary material related to this article can be found, in the online version, at doi:<https://doi.org/10.1016/j.cherd.2022.01.036>.

References

- Abrams, D.S., Prausnitz, J.M., 1975. Statistical thermodynamics of liquid mixtures: a new expression for the excess Gibbs energy of partly or completely miscible systems. *AIChE J.* 21, 116–128.
- AMACS Process Tower Internals, 2020. *AMACS Fractionation Trays*.
- Caballero, J.A., 2015. Logic hybrid simulation-optimization algorithm for distillation design. *Comput. Chem. Eng.* 72, 284–299.
- Caballero, J.A., Milán-Yañez, D., Grossmann, I.E., 2005. Rigorous design of distillation columns: integration of disjunctive programming and process simulators. *Ind. Eng. Chem. Res.* 44, 6760–6775.
- Chuang, K.T., Nandakumar, K., 2000. Tray columns: design. *Distillation Tray Columns Des.* 1, 1135–1140.
- Cicalese, J.J., Davis, J.A., Harrington, P.J., Houghland, G.S., Hutchinson, A.J.L., Walsh, T.J., 1947. Study of alkylation-plant isobutane tower performance. *Pet. Ref.* 495.
- Couper, J.R., Penney, W.R., Fair, J.R., Walas, S.M., 2012. Distillation and gas absorption. In: Couper, J.R., Penney, W.R., Fair, J.R., Walas, S.M. (Eds.), *Chemical Process Equipment: Selection and Design*. Butterworth-Heinemann, Boston, pp. 399–486.
- Dowling, A.W., Biegler, L.T., 2015. A framework for efficient large scale equation-oriented flowsheet optimization. *Comput. Chem. Eng.* 72, 3–20.
- Dutta, B.K., 2007. *Principles of Mass Transfer and Separation Processes*. PHI Learning Pvt. Ltd., New Delhi.
- Economopoulos, A.P., 1978. Computer design of sieve trays and tray columns. *Chem. Eng.* 85, 109–120.
- Eduljee, H.E., 1959. Design of sieve-type distillation plates. *Br Chem Eng* 320.
- Engel, V., 2020. How to...sieve tray: how to design and optimize sieve trays. *WelChem Process Technol.*
- Fair, J.R., 1961. How to predict sieve tray entrainment and flooding. *Petro/Chem Eng* 33, 45–52.
- Fair, J.R., 1963. Tray hydraulics: perforated trays. In: Smith, B.D. (Ed.), *Design of Equilibrium Stage Processes*. McGraw-Hill, New York, pp. 539–569.
- Gradshteyn, I.S., Ryzhik, I.M., 2015. *Table of Integrals, Series, and Products*, 8th ed. Elsevier, London.
- Humphrey, J., 1995. Separation processes: playing a critical role. *Chem. Eng. Prog.* 91, 43–54.
- Hunt, C.D., Hanson, D.N., Wilke, C.R., 1955. Capacity factors in the performance of perforated-plate columns. *AIChE J.* 1, 441–451.
- Ibrahim, D., Jobson, M., Guillén-Gosálbez, G., 2017. Optimization-based design of crude oil distillation units using rigorous simulation models. *Ind. Eng. Chem. Res.* 56, 6728–6740.
- Javaloyes-Antón, J., Ruiz-Femenia, R., Caballero, J.A., 2013. Rigorous design of complex distillation columns using process simulators and the particle swarm optimization algorithm. *Ind. Eng. Chem. Res.* 52, 15621–15634.
- Kister, H.Z., 1990. *Distillation Operation*. McGraw-Hill, Inc, New York.
- Kister, H.Z., 1992. *Distillation Design*. McGraw-Hill, Inc, New York.
- Kong, L., Maravelias, C.T., 2019. From graphical to model-based distillation column design: a McCabe-Thiele-inspired mathematical programming approach. *AIChE J.* 65, 1–11.
- Kooijman, H.A., Taylor, R., 2006. In: Kooijman, H.A., Taylor, R. (Eds.), *The ChemSep Book*, 2nd ed.
- Lahiri, S.K., 2014. Particle swarm optimization technique for the optimal design of plate-type distillation column. In: Valadi, J., Siarry, P. (Eds.), *Applications of Metaheuristics in Process Engineering*. Springer, New York, pp. 153–182.
- Lahiri, S.K., 2020. New design methodology. In: *Profit Maximization Techniques for Operating Chemical Plants*. John Wiley & Sons, Ltd, Hoboken, pp. 231–257.
- Lygeros, A.I., Magoulas, K.G., 1986. Column flooding and entrainment. *Hydrocarbon Process*, 65.
- Lyu, H., Cui, C., Zhang, X., Sun, J., 2021. Population-distributed stochastic optimization for distillation processes: implementation and distribution strategy. *Chem. Eng. Res. Des.* 168, 357–368.
- Oberg, E., Jones, F.D., Horton, H.L., Ryffel, H.H., 2004. *Machinery's Handbook*, 27th ed. Industrial Press Inc., New York.
- Ogboja, O., Kuye, A., 1990. A procedure for the design and optimization of sieve trays. *Chem. Eng. Res. Des.* 68, 445–452.
- Plouffe, S., 2001. *The First 498 Bernoulli Numbers*. Project Gutenberg, Champaign.
- Redlich, O., Kwong, J.N.S., 1979. On the thermodynamics of solutions V. An equation-of-state. Fugacities of gaseous solutions. *Chem. Rev.* 44, 223–244.
- Towler, G., Sinnott, R., 2013. *Chemical Engineering Design Principles: Practice and Economics of Plant and Process Design*, 2nd ed. Elsevier, Oxford.
- Viswanathan, J., Grossmann, I.E., 1993. An alternate MINLP model for finding the number of trays required for a specified separation objective. *Comput. Chem. Eng.* 17, 949–955.
- Wankat, P.C., 1988. *Separations in Chemical Engineering: Equilibrium Staged Separations*. Elsevier, New York.
- Yeoh, K.P., Hui, C.W., 2021. Rigorous NLP distillation models for simultaneous optimization to reduce utility and capital costs. *Clean. Eng. Technol.* 2, 100066.
- Yeomans, H., Grossmann, I.E., 2000. Disjunctive programming models for the optimal design of distillation columns and separation sequences. *Ind. Eng. Chem. Res.* 39, 1637–1648.

Glossary

Nomenclature

Aa: Active area (m²)

Aap: Clearance area under the downcomer (m^2)
Ac: Total column area (m^2)
Acz: Calming zone area (m^2)
Adc: Downcomer area (m^2)
Ah: Total area of all the active holes (m^2)
An: Vapor flow area (m^2)
Asector: Circular sector area (m^2)
Atriangle: Triangle area (m^2)
Aus: Unperforated strip area (m^2)
Be: Bernoulli number
Co: Orifice coefficient
Csb: Sounders-Brown coefficient (m/s)
Ctotal: Total column cost (\$)
 $\hat{C}w$: Factor of cost equation (dimensionless)
Dc: Column diameter (m)
dh: Hole diameter (m)
Dm: Mean diameter of column (m)
FAdc: Factor of downcomer area (%)
Fflood: Factor of flooding (dimensionless)
Flv: Liquid-vapor flow factor (dimensionless)
hap: Height of the clearance under the downcomer (m)
hb: Height of the downcomer backup (m)
Hc: Height of column between tangent lines (m)
hd: Dry tray head loss (m)
hdc: Head loss in the downcomer (m)
Hdc: Height of downcomer (m)
hdwap: Difference between weir and clearance height under the downcomer (m)
how: Height of the liquid crest over the weir (m)
 $\hat{h}r$: Residual head loss (m)
ht: Total tray head loss (m)
hw: Weir height (m)
K1: Parameter of the Fair's flooding correlation (dimensionless)
K2: Parameter of the weeping correlation (dimensionless)
lay: Hole layout
lcz_{in}: Length of the inlet calming zone (m)
lcz_{out}: Length of the outlet calming zone (m)
lp: Hole pitch (m)
lt: Tray spacing (m)
lw: Weir length (m)
 $\dot{L}w$: Liquid mass flow rate (kg/s)
 $\hat{N}t$: Number of trays
 $\hat{p}Dc$: Available values of the column diameter (m)
 $\hat{p}dh$: Available values of the hole diameter (m)
 $\hat{p}lay$: Available values of the hole layout
 $\hat{p}lp$: Available values of the hole pitch (m)
 $\hat{p}lt$: Available values of the tray spacing (m)
 $\hat{p}lw$: Available values of the weir length (m)
 $\hat{p}hdwap$: Available values of the difference between weir and clearance height under the downcomer (m)
 $\hat{p}hw$: Available values of the weir height (m)
 $\hat{p}tt$: Available values of the tray thickness (m)
 $\hat{p}twall$: Available values of the wall thickness (m)
time: Residence time (s)
tt: Tray thickness (m)
twall: Column wall thickness (m)
uflood: Flooding velocity (m/s)
uh: Flow velocity throughout the tray holes (m/s)
uhmin: Minimum vapor flow velocity (m/s)
un: Vapor flow velocity (m/s)

Vt: Volume of the tray deck (m^3)
 $\dot{V}w$: Vapor mass flow rate (kg/s)
Vwdc: Volume of the combination weir/downcomer (m^3)
 $\hat{w}cz_{in}$: Width of inlet calming zone (m)
 $\hat{w}cz_{out}$: Width of outlet calming zone (m)
Wcolumn: Mass of the column shell and internals (kg)
Wshell: Mass of the column shell (kg)
Wt: Mass of the trays (kg)
Wtotal: Mass of the distillation column (kg)
wus: Width of the unperforated strip (m)
yDc: Binary variable of the column diameter
ydh: Binary variable of the hole diameter
yhwap: Binary variable of the difference between weir and clearance height under the downcomer
yK1: Binary variable of the K1 parameter
y_{lay}: Binary variable of the hole layout
y_{lp}: Binary variable of the hole pitch
y_{lt}: Binary variable of the tray spacing
y_{lw}: Binary variable of the weir length
y_{tt}: Binary variable of the tray thickness
y_{wus}: Binary variable of the width of the unperforated strip

Greek symbols

α : Active area angle (rad)
 β : Calming zone angle (rad)
 δ : Ratio between the weir length and the column diameter (dimensionless)
 $\hat{\epsilon}$: Small positive valor equal to 10^{-6}
 θ : Weir angle (rad)
 $\hat{\rho}l$: Specific mass of liquid (kg/m^3)
 $\hat{\rho}shell$: Specific mass of shell material (kg/m^3)
 $\hat{\rho}t$: Specific mass of tray material (kg/m^3)
 $\hat{\rho}v$: Specific mass of vapor (kg/m^3)
 $\hat{\rho}w$: Specific mass of carbon steel (kg/m^3)
 σ : Surface tension (N/m)
 ϕ : Ratio between the hole diameter and the hole pitch (dimensionless)
 ψ : Fractional entrainment (kg/kg gross liquid flow)
 ω : Ratio between the tray thickness and the hole diameter (dimensionless)

Subscripts

in: Inlet
out: Outlet
min: Lower bound
max: Upper bound
sDc: Set of column diameter
sdh: Set of hole diameter
shdwap: Set of difference between weir and clearance height under the downcomer
shw: Set of weir height
sK1: Set of the K1 constant
slp: Set of hole pitch
slt: Set of tray spacing
slw: Set of weir length
sNt: Set of column trays
swczout: Set of the width of outlet calming zone
swus: Set of the width of unperforated strip